NRC Research Press

ARTICLE

Characterization of an alluvial silt and clay deposit for monotonic, cyclic, and post-cyclic behavior

Karina R. Dahl, Jason T. DeJong, Ross W. Boulanger, Robert Pyke, and Douglas Wahl

Abstract: This paper presents a detailed characterization of the monotonic, cyclic, and post-cyclic behavior of two strata within a recent Holocene alluvial deposit of silty sand, sandy silt, silt, and clay. Stratum A is composed predominantly of very soft clay and very loose silt with plasticity indices ranging from 5 to 27, whereas stratum B is composed predominantly of very loose silty sand and sandy silt with plasticity indices ranging from 0 to 10. Characterization included in situ testing, undisturbed soil sampling and laboratory testing, and a field surcharge test section. Consolidation tests and monotonic, cyclic, and post-cyclic direct simple shear tests were used to evaluate the effects of varying the consolidation stress, consolidation stress history, and initial static shear stress ratio. The field and laboratory test data show distinct differences in behavior between the two soil strata, which can be related to their different index test characteristics. These results are compared with their respective behaviors predicted using common engineering correlations. The field and laboratory test data summarized herein contribute to the database and understanding of the monotonic, cyclic, and post-cyclic behaviors of low-plasticity fine-grained soils.

Key words: silt, clay, cyclic strength, liquefaction, earthquakes.

Résumé : Cet article présente une caractérisation détaillée du comportement monotonique, cyclique et post-cyclique de deux strates à l'intérieur d'un dépôt alluvial datant de l'Holocène récent, fait de silt sablonneux, de sable silteux, de silt et d'argile. La strate A est composée principalement d'argile très molle et de silt très lâche avec des indices de plasticité variant entre 5 et 27, tandis que la strate B est faite principalement de sable silteux très lâche et de silt sablonneux avec des indices de plasticité entre 0 et 10. Les travaux de caractérisation comprenaient des essais in-situ, l'échantillonnage de sols intacts et des essais au laboratoire, de même qu'une section d'essai de terrain en surcharge. Les essais de consolidation et les essais de cisaillement simple direct monotoniques, cycliques et post-cycliques ont été utilisés pour évaluer les effets de la variation de la contrainte de consolidation, de l'historique des contraintes de consolidation et du ratio des contraintes de cisaillement statiques initiales. Les données des essais de terrain et de laboratoire ont démontré des différentes marquées de comportement entre les deux strates de sol, qui peuvent être reliées à leurs caractéristiques indices différentes. Ces résultats sont comparés à leurs comportements respectifs prédits à l'aide de corrélations typiques en ingénierie. Les données d'essais de terrain et de laboratoire résumées dans cet article contribuent à la base de données et à la compréhension des comportements monotoniques, cycliques et post-cycliques de sols fins à faible plasticité. [Traduit par la Rédaction]

Mots-clés : silt, argile, résistance cyclique, liquéfaction, séismes.

Introduction

Current practice for evaluating potential strength loss and deformation in low-plasticity fine-grained soils begins with an evaluation of their susceptibility to liquefaction. Cyclic strengths for fine-grained soils deemed liquefiable are most commonly evaluated using case history–based standard penetration test (SPT) and cone penetration test (CPT) liquefaction correlations, although it is recognized that the fundamental and empirical bases for the influence of fine-grain characteristics on such correlations are not well developed. Cyclic strengths for fine-grained soils that are deemed nonliquefiable can be evaluated using methods that are similar to those for measuring their monotonic undrained strengths (s_u), including in situ tests, laboratory tests, and laboratory-based correlations relating monotonic and cyclic strengths (e.g., Boulanger and Idriss 2007). Bray and Sancio (2006) developed liquefaction susceptibility criteria in terms of plasticity index (PI) and water content (w_c) to liquid limit (LL) ratios, based on observations of field performance and laboratory testing of field samples from sites affected by the 1999 Kocaeli earthquake in Adapazari, Turkey. Boulanger and Idriss (2006) developed liquefaction susceptibility criteria in terms of PI, with the criteria guiding the recommended choice of engineering procedures for evaluating the seismic behavior of fine-grained soils. Still, there are a limited number of laboratory studies on low-plasticity silts (e.g., Yilmaz et al. 2004; Sanin and Wijewickreme 2006) and even fewer cases (e.g., Boulanger et al. 1998; Bray and Sancio 2006; Sanin and Wijewickreme 2006) that integrate information from in situ testing, advanced laboratory testing, and field performance to describe the expected response of such soils to seismic loading. Additional detailed case studies will be essential for the further development of engineering procedures for evaluating the seismic behavior of low-plasticity fine-grained soils.

This paper summarizes the results of a detailed laboratory characterization of soil behavior for an alluvial deposit of silty sand, sandy silt, silt, and clay in California. The recent Holocene alluvium at the study site includes an upper stratum of very soft clay

Received 9 February 2013. Accepted 10 January 2014.

K.R. Dahl. Damwatch Services Ltd., Wellington, NZ.
J.T. DeJong and R.W. Boulanger. Department of Civil and Environmental Engineering, University of California, Davis, CA 95616, USA.
R. Pyke. Walnut Creek, CA 94549, USA.
D. Wahl. GeoPentech, Santa Ana, CA 92701, USA.
Corresponding author: Ross W. Boulanger (e-mail: rwboulanger@ucdavis.edu).

to very loose silt (referred to as stratum A) overlying a stratum of loose sandy silt to silty sand (referred to as stratum B). The soils within these two strata have characteristics (e.g., PI from 0 to 27) that span the margins of currently available liquefaction susceptibility criteria, and thus a laboratory testing program was performed to guide the selection of appropriate engineering properties and analysis procedures. The site characterization work presented herein was part of a comprehensive evaluation of the static and seismic performance of engineered fills proposed for the site, including the potential benefits of surcharge preloading and other mitigation efforts. The site characterization work included in situ testing (borings with SPTs, CPTs, and vane shear tests (FVT)), undisturbed soil sampling and laboratory testing (index, consolidation, and monotonic, cyclic, and post-cyclic direct simple shear (DSS) tests), and a field surcharge test section. The field and laboratory test data show a distinct difference in soil behavior between the two soil strata. Results are presented to illustrate these differences, including the effects of consolidation stress, consolidation stress history, and initial static shear stress ratio. Full details of the experimental work are given in Dahl (2011). The field and laboratory data are compared with behaviors predicted using common engineering correlations. Synthesis of site-specific in situ, laboratory, and field test data proved beneficial, relative to the use of generalized design procedures, for evaluating the static and seismic performance of proposed fills at this site.

Site conditions

The study site is located at the western end of Potrero Canyon, a narrow 5.5 km long valley about 15 km northwest of San Fernando Valley in Los Angeles County. Soil profiles within the valley typically consist of about 12 m of recent Holocene alluvial gravel, sand, silt, and clay overlying older dense silty sand and firm lean clay (Bennett et al. 1998). Rymer et al. (1995) reported observations of ground cracking along the margins of the canyon during the 1994 Northridge earthquake (M_w = 6.7) with most cracks having at least 10 cm extensional displacement (Rymer et al. 1995). Holzer et al. (1999) estimated that the peak ground acceleration in this area was ~0.35*g* and concluded that ground deformations along the canyon margins were due primarily to liquefaction of Holocene sand lenses within the upper alluvium at those locations. The study site was approximately level and located near the center of the canyon, away from the margins of the valley where ground movements were observed. This suggests that any ground deformations at the study site were at least small enough to not attract the attention of field reconnaissance teams. Engineering studies showed that deformation analysis results were reasonably consistent with the observed ground cracking patterns at the margins of the canyon and the inferred range of possible movements near the canyon center, but the details of those studies are beyond the scope of this paper. A 7.6 m high test fill with a footprint 56 m by 43 m was constructed at the study site to evaluate potential consolidation settlements under proposed fills. This paper summarizes the characterization of the soils at the study site for the purpose of designing proposed site developments.

Field investigations included SPTs, CPTs, FVTs, and sampling using ~76 mm diameter Shelby tubes with an Osterberg piston sampler. Samples were obtained from below the test fill at depths of 1.25 to 3.44 m below original ground surface and ~90 m outside the fill footprint at depths of 4.85 to 5.39 m. The profile and in situ test data are summarized in Fig. 1.

The subsurface soil profile (Fig. 1) consists of a ~1 m thick layer of surficial material (desiccated clay and silt), overlying a 3.1 to 3.4 m thick layer of very soft clay to very loose silt (i.e., stratum A), overlying a 4 m thick layer of loose sandy silt to silty sand (i.e., stratum B). The underlying soil layer between depths of ~8.2 and 13.0 m consists primarily of stiff to very stiff silty clays and clayey silts with 0.5 to 0.8 m thick interlayers of medium dense to dense

Fig. 1. Typical subsurface conditions and CPT, SPT, and FVT profiles. N_{60}, energy-corrected SPT blow count; OG, original ground surface; q_t, cone tip resistance; σ_{vo}, in situ vertical stress; σ'_{vo}, in situ vertical effective stress; τ_{peak}, undrained peak shear strength.

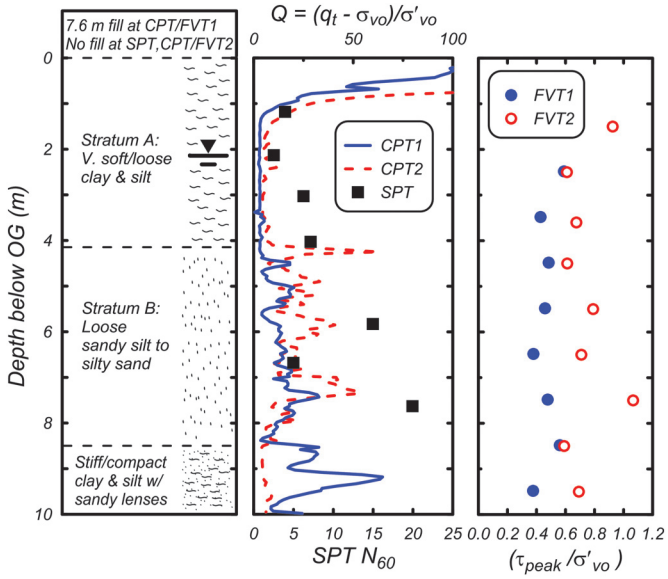

silty sand and sandy silt. Depth to the groundwater table varies seasonally from 2.1 to 5.6 m (Bennett et al. 1998) and was at 2.1 m depth during the field investigations.

Stratum A soils classify predominantly as low-plasticity clay (CL) and silt (ML), and occasionally as fat clay and elastic silt (CH and MH) per the Unified Soil Classification System (USCS; ASTM 2011) (Fig. 2). The stratum is fairly uniform, with the sampled soils generally having fines content greater than 93%, clay content (<0.002 mm) of 26% to 34%, water content of 30% to 34%, and a PI of 5 to 27 (average of 18).

Stratum B soils classify as silty sand (SM) and sandy silt (ML). The soils in the sampling interval generally have fines content of 35% to 77%, clay content of 9% to 23%, and water content of 20% to 30%. Soils classifying as silty sand (fines content of 35% to 50%) generally have a PI less than 2, whereas soils classifying as sandy silt (fines content of 50% to 77%) generally have a PI between 3 and 10. These SM and ML soils are finely interlayered, have smooth transitions across soil types, and are visually difficult to distinguish between. It was suspected that the behavior of both soil types may be dominated by the fines fraction, but test results shown later do show differences in behavior across this range of gradations.

Consolidation behavior

Incremental load (ICL) and constant rate of strain (CRS) consolidation tests were performed on samples from each stratum. Samples were trimmed to a diameter of 64 mm and a height of 25.4 mm for testing. For stratum A samples obtained beneath the test fill, the estimated preconsolidation stresses (σ'_p) were ≈160–200 kPa (e.g., Fig. 3), which are comparable to the estimated in situ vertical effective stresses (σ'_{vo}) of 170 to 200 kPa. These results are consistent with the observed large settlements of the test fill and with previous test data indicating that fill placement would bring the stratum to a normally consolidated state. For stratum B samples obtained outside the test fill area, the estimated σ'_p values were ≈80–95 kPa (e.g., Fig. 3), which are slightly greater than the estimated σ'_{vo} ≈ 64 kPa. These data indicate the soils are slightly overconsolidated outside the test fill area, as expected.

The coefficient of consolidation, c_v, from ICL tests ranged from 0.003 to 0.18 cm²/s for stratum A specimens and from 0.014 to

Fig. 2. Atterberg limits of strata A and B specimens. FC, fines content.

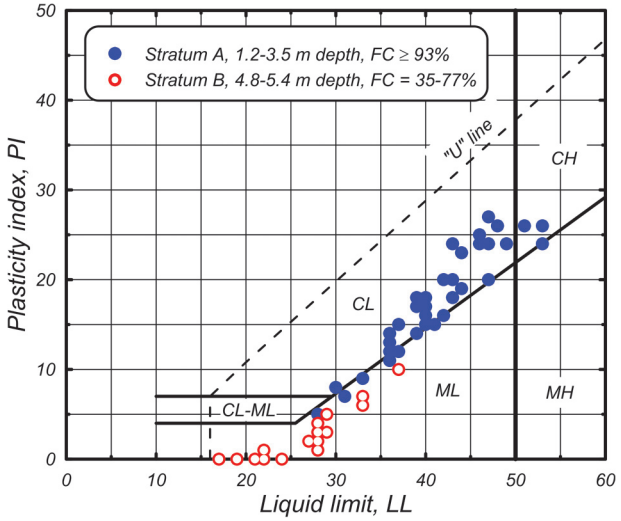

Fig. 3. CRS and ICL consolidation curves for strata A and B specimens.

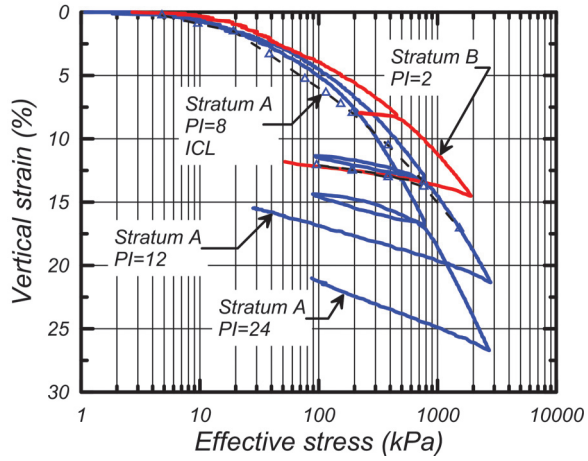

0.064 cm²/s for stratum B specimens. Inverse analyses of the test fill's settlement measurements, assuming that the two strata have the same c_v value, indicate an average c_v of ≈0.11 cm²/s. The field estimate of c_v is slightly greater than the average values obtained in the laboratory consolidation tests, which is consistent with the expected effects that coarser lenses and interlayers within the two strata would have on full-scale response.

The sample quality designation (SQD) methods by Terzaghi et al. (1996) and Lunne et al. (1997) generally indicate low sample qualities. This may be due to difficulty obtaining high-quality samples in low-plasticity silts and sandy silts, or it may indicate that these criteria, developed primarily for soft cohesive soils with PI ≥ 25, are not directly applicable to low-plasticity silts and sandy silts. Concerns with low sample quality ratings are mitigated for the present study by the fact that future loading conditions (new fills) will increase the effective stresses to values much greater than currently exist and thus monotonic and cyclic tests at these larger stresses will be less affected by sampling disturbance.

Monotonic undrained loading

Monotonic undrained DSS tests on specimens trimmed to 66 mm diameter and 18 mm height were performed with a

Fig. 4. Stress–strain response for strata A and B specimens during undrained monotonic DSS loading.

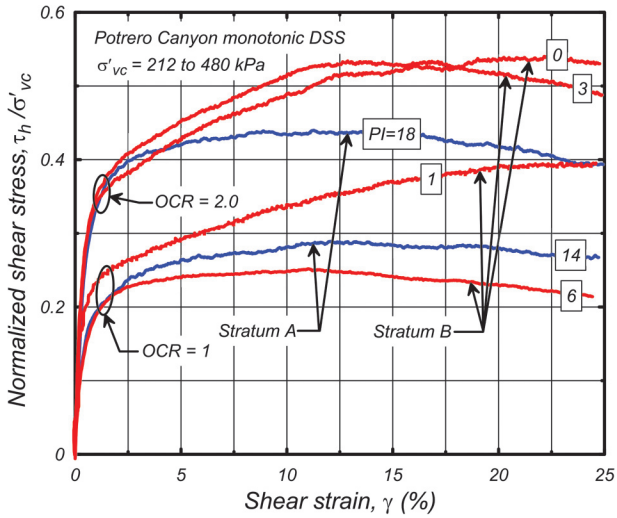

GEOTAC DigiShear DSS apparatus using a latex membrane around the specimen that is confined to zero lateral strain by sixteen 1.6 mm thick stacked rings. The DSS device is configured for constant-volume (constant-height) shear loading. Monotonic tests were performed at strain rates of 5%/h (duration <300 min) unless otherwise noted. Stratum A specimens were consolidated to a vertical effective stress $\sigma'_{vc} = 1.2\sigma'_{vo}$ (ranging from 212 to 240 kPa) and $2.4\sigma'_{vo}$ (~440 kPa), both of which correspond to normally consolidated conditions (overconsolidation ratio OCR = 1). Another set of stratum A specimens were consolidated to $\sigma'_{vc} = 2.4\ \sigma'_{vo}$ (ranging from 440 to 480 kPa) followed by unloading to $1.2\sigma'_{vo}$ (ranging from 220 to 240 kPa), which corresponds to an OCR of 2.0. Parallel sets of tests on stratum B specimens used similar consolidation stresses as those for stratum A specimens, which resulted in laboratory stresses that greatly exceed the in situ consolidation stresses for stratum B specimens from outside the fill area.

Representative results of monotonic undrained DSS tests on strata A and B specimens with OCR of 1.0 and 2.0 are presented in Fig. 4. Normalized shear stress (τ_h/σ'_{vc}) versus shear strain (γ) responses are shown for γ up to 25%, but it should be recognized that stress nonuniformities at large γ values in DSS devices can strongly influence the stress–strain response, such that they do not necessarily represent the true soil behavior (DeGroot et al. 1994). Stratum A specimens exhibited nearly constant shear resistances between γ of 5% and 20%, with normalized undrained strengths (s_u/σ'_{vc}) of 0.24 to 0.29 for OCR = 1 regardless of consolidation stress and 0.44 to 0.53 for OCR = 2.0. These data can be expressed in the form (Ladd and Foott 1974)

$$(1) \qquad \frac{s_u}{\sigma'_{vc}} = S(\mathrm{OCR}^m)$$

where S is the value of s_u/σ'_{vc} for OCR = 1, and m is the slope of the s_u/σ'_{vc} versus OCR relationship on a log–log plot. Data for stratum A specimens results in $S = 0.27$ and $m = 0.86$, which are within the range of values that Ladd (1991) summarized for ordinary sedimentary clays. These results indicate that stratum A soils are amenable to a stress history normalization of their engineering properties.

The responses of the stratum B specimens showed some notable differences from those for stratum A specimens, depending on the specimen's PI. Stratum B specimens with PI ≤ 3 exhibited a slight strain-hardening response after they transitioned from in-

Fig. 5. Stress–strain response and effective stress path for (*a*) stratum A and (*b*) stratum B specimens during undrained cyclic DSS loading.

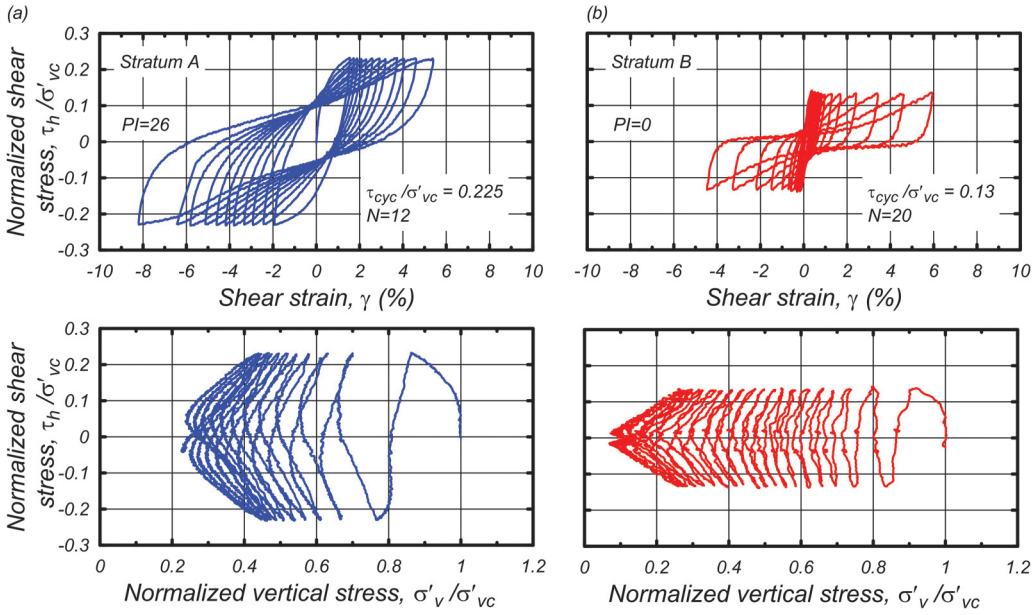

crementally contractive to incrementally dilative behavior at $\gamma \approx$ 4%–5% (e.g., a phase transformation behavior that is often associated with cohesionless soils). These specimens continued to strain harden up to $\gamma \approx 15\%$, regardless of OCR, and eventually developed normalized shear resistances that were roughly 20%–30% greater than those for stratum A specimens. In contrast, the stratum B specimen with PI = 6 and OCR = 1 exhibited a nearly perfectly plastic response and a normalized shear resistance that is similar to those for the stratum A specimens. The stratum B specimens exhibited an increase in s_u with increasing OCR that is similar to that observed for stratum A specimens. Altogether, however, the application of a "stress history and normalized soil engineering properties" (SHANSEP)-type procedure to the results for stratum B is complicated by the difficulty in defining s_u for the strain-hardening responses of the lower-plasticity specimens.

The effect of consolidation under an initial horizontal static shear stress ratio (τ_{st}/σ'_{vc}) of 0.05 on subsequent monotonic undrained DSS loading behavior was evaluated in two additional tests on stratum A specimens with an OCR of 1.0 and 2.0. The undrained stress–strain responses and s_u/σ'_{vc} ratios were similar to those for specimens consolidated under $\tau_{st}/\sigma'_{vc} = 0.0$, within the range of test variability (Dahl 2011).

Comparison with in situ test results

FVT results in stratum A produced undrained peak shear strength ratios (τ_{peak}/σ'_{vo}) of 0.43 and 0.59 beneath the test fill (FVT1 in Fig. 1) and 0.61 to 0.93 outside the test fill area (FVT2 in Fig. 1). Stratum A is normally consolidated under the test fill and lightly overconsolidated outside the test fill, such that the differences in the τ_{peak}/σ'_{vo} values from beneath the test fill to outside the test fill are reasonable. The FVT τ_{peak}/σ'_{vo} values under the test fill are, however, about twice as high as the values obtained from the monotonic undrained DSS tests (i.e., $s_u/\sigma'_{vc} = 0.27$) or those typically expected for normally consolidated clay. FVT torque versus rotation records were inspected for any signs of local sand lenses having caused an overestimation of strengths, but the records included no evidence of unusual torque–rotation behaviors. The potential for partial drainage to have caused the higher FVT strengths was evaluated using the relationships in Chandler (1988); for the 55 mm diameter vane at typical rotation rates, an average degree of consolidation greater than 10% would be expected for c_v values greater than ~0.02 cm²/s. The c_v values from the consolidation tests and the back-analysis of the test fill settlements, as discussed previously, are sufficiently large to suggest that partial drainage around the vane may have contributed to the unexpectedly high FVT strengths.

CPT tip resistances in stratum A produced s_u/σ'_{vc} values that were typically 0.24 to 0.29 (with local intervals as high as 0.35 to 0.44) beneath the test fill and typically 0.38 to 0.53 outside the test fill, based on a cone bearing factor (N_k) of 12. Lunne and Kleven (1981) showed the value of N_k as ranging between 11 to 19 (average of 15) for normally consolidated marine clays when using results of FVT as a reference. For the CPT, estimates of s_u may be affected by partial drainage when the c_v value is greater than ~0.10 cm²/s (Hight and Leroueil 2003) to 0.24 cm²/s (Randolph 2004). In this case, the estimated c_v values suggest that partial drainage did not significantly affect the CPT results, despite having affected the FVT results.

FVT and CPT results in stratum B both indicated s_u/σ'_{vc} values significantly greater than measured in the laboratory or estimated by empirical relationships; e.g., beneath the test fill, the FVT produced τ_{peak}/σ'_{vo} of 0.38 to 0.48 and the CPT produced s_u/σ'_{vc} of 0.33 to 0.93. The FVT and CPT strengths appear to have been strongly affected by partial drainage and (or) sand interlayers within this stratum.

Cyclic undrained loading

Cyclic undrained DSS tests were performed on 21 stratum A specimens (PI ≥ 5) and nine stratum B specimens (PI ≤ 10). Specimens were consolidated to the same stresses and OCR values as for the monotonic undrained DSS tests. Select samples were consolidated with τ_{st}/σ'_{vc} of 0.02, 0.05 or 0.10 to simulate the effects of a sloping ground surface. Uniform cyclic stress ratios (τ_{cyc}/σ'_{vc}) were applied under strain-controlled loading at a strain rate of 50%/h. The frequency of the resulting stress–time series varied with strain level; e.g., cycles with shear strain amplitudes of 0.1% and 1.0% had frequencies of 0.035 and 0.0035 Hz, respectively.

Typical responses of normally consolidated (OCR = 1) strata A and B specimens are shown in Figs. 5*a* and 5*b*. The stratum A specimen loaded at $\tau_{cyc}/\sigma'_{vc} = 0.225$ reached a peak single-amplitude shear strain (γ_{peak}) of 3% at four cycles and 5% at eight cycles. This specimen produced wide hysteretic loops and reached a maximum excess pore pressure ratio ($r_u = \Delta u/\sigma'_{vc}$) of 0.78. The stratum B

specimen (with PI = 0) loaded at τ_{cyc}/σ'_{vc} = 0.130 reached a γ_{peak} of 3% at 18 cycles and 5% at 20 cycles. This specimen produced narrower hysteretic loops and reached a higher maximum r_u of 0.93.

The rate of pore pressure generation for specimens from each stratum are compared in Fig. 6, showing the maximum r_u versus peak single-amplitude shear strain (γ_{peak}) for different numbers of loading cycles. The maximum r_u for specimens from either stratum increases with increasing γ_{peak}, and to a lesser degree increases with increasing number of loading cycles required to reach a given γ_{peak}. The dependence of this r_u versus γ_{peak} relationship on number of loading cycles indirectly reflects the combined influence of the imposed cyclic stress ratio (smaller cyclic stress ratios require more cycles to reach a given γ_{peak}) and cumulative energy dissipation (smaller cyclic stress ratios require greater energy dissipation to reach a given γ_{peak}). Stratum B specimens consistently reached higher maximum r_u values than stratum A specimens for the same γ_{peak} and number of loading cycles. For example, stratum A specimens reached maximum r_u values of ~0.45–0.70 at γ_{peak} = 3% whereas stratum B specimens reached maximum r_u values of ~0.75–0.90 at the same γ_{peak}. The higher maximum r_u values for stratum B specimens are consistent with them having lower fines content and PI than stratum A.

The combinations of τ_{cyc}/σ'_{vc} and number of uniform stress cycles (N) causing γ_{peak} = 3% are summarized in Fig. 7 for stratum A specimens and Fig. 8 for stratum B specimens. This strain criterion is consistent with the cyclic failure criterion used by Idriss and Boulanger (2008). Results were fitted as

$$\text{CRR} = aN^{-b} \quad (2)$$

where the cyclic resistance ratio (CRR) is the τ_{cyc}/σ'_{vc} required to reach the specified failure criterion in N cycles, and a and b are fitting parameters. The fitted parameters are summarized on the figures. The cyclic test results for stratum A specimens (Fig. 7), all which had PI ≥ 7, show a strong influence of OCR; for example, the CRR to γ_{peak} = 3% in 10 cycles increases from about 0.20 at OCR = 1 to about 0.35 at OCR = 2.0. This increase in CRR is comparable to the previously described increase in s_u for the same increase in OCR. The slope of the CRR versus N relationship is lower for the OCR = 1 specimens (b = 0.047) than for the OCR = 2.0 specimens (b = 0.090). Both slopes are reasonably consistent with results reported for other cohesive soils (e.g., b = 0.07 to 0.15 in Boulanger and Idriss 2007).

Cyclic tests results for the two highest plasticity specimens from stratum B (PI = 7 at OCR = 1, and PI = 10 at OCR = 2.0) are plotted with the stratum A results in Fig. 7. The CRR for these two Stratum B specimens plot slightly lower than the results for stratum A specimens, despite these specimens having comparable PI values. The slightly lower CRR values for these two stratum B specimens may be attributed to other differences in the specimen characteristics, including the fact these stratum B specimens have lower fines contents (61%–77%) than the stratum A specimens (93%–96%).

Cyclic test results for the other stratum B specimens (Fig. 8), all which had PI ≤ 2, indicate lower CRR values than were obtained for the stratum A soils; for example, the CRR to γ_{peak} = 3% in 10 cycles for OCR = 1 was about 0.15 for stratum B soils versus about 0.20 for stratum A soils. The slope of the CRR versus N relationship is steeper for the stratum B specimens (b = 0.139 at OCR = 1) than for the stratum A specimens (b = 0.047 at OCR = 1), which is consistent with these stratum B specimens being almost nonplastic. The stratum B specimens suggest a similarly strong influence of OCR, although only two tests were performed with OCR = 2.0 and one of those was a more plastic specimen. The results for the two higher plasticity stratum B specimens, also shown on Fig. 8, produced slightly higher CRR values than those for the lower plasticity stratum B specimens.

Fig. 6. Excess pore pressure generated relationship to number of cycles and peak shear strain for strata A and B specimens.

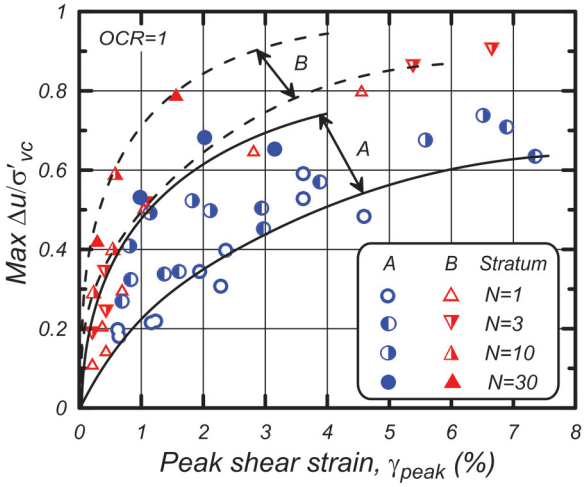

Fig. 7. Cyclic stress ratios to cause cyclic failure versus number of uniform loading cycles for normally consolidated and OCR = 2.0 stratum A specimens.

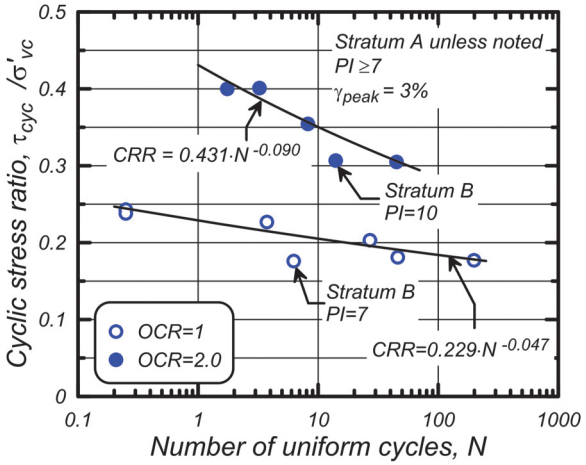

Fig. 8. Cyclic stress ratios to cause cyclic failure versus number of uniform loading cycles for normally consolidated and OCR = 2.0 stratum B specimens.

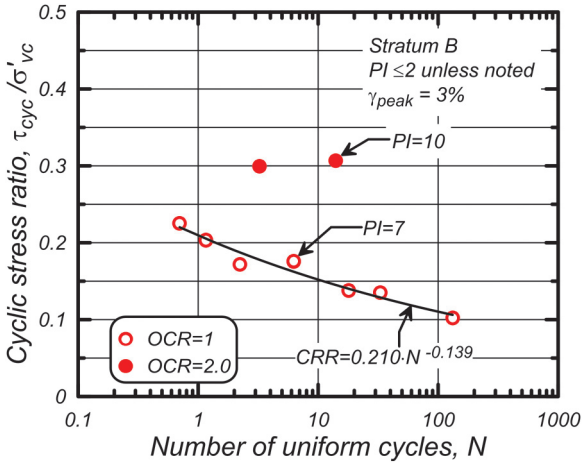

Fig. 9. Cyclic strength ratios to cause cyclic failure versus number of uniform loading cycles for normally consolidated and OCR = 2.0 stratum A specimens.

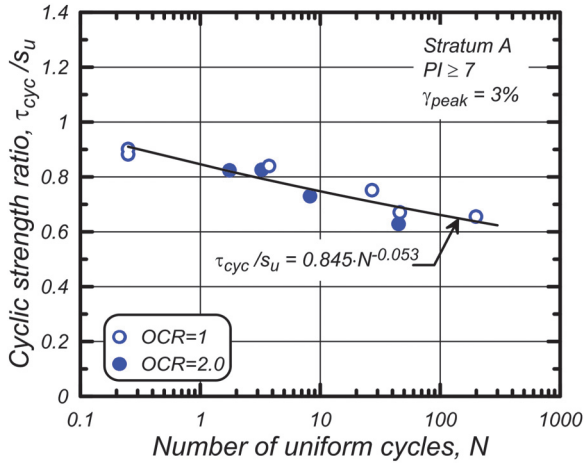

Normalization of cyclic strengths by undrained shear strengths

The cyclic test data for stratum A specimens with OCR = 1.0 and 2.0 are shown in Fig. 9 in terms of the cyclic strength ratio (τ_{cyc}/s_u) versus N causing γ_{peak} = 3%. The τ_{cyc}/s_u values are slightly greater for OCR = 1.0 specimens than for OCR = 2.0 specimens, but the differences are not significant. The combined set of data produces an average τ_{cyc}/s_u of 0.71 at 30 cycles, which is at the lower range of reported values (0.71 to 0.92) for DSS loading of natural silts and clays (Boulanger and Idriss 2007). The relatively low τ_{cyc}/s_u for stratum A specimens may be partly attributed to (*i*) the slower cyclic loading rates used in these tests and (*ii*) the samples having only recently been loaded into a normally consolidated condition under the test fill, which may have partly erased any benefits of in situ aging, thixotropy or cementation for these soft sediments.

Cyclic strength ratios for stratum B specimens are more difficult to define because these soils exhibited strain-hardening responses in monotonic undrained shearing. One option would be to define s_u as corresponding to some specified γ, but this approach was found to be sensitive to the selected value of γ; e.g., a larger γ criterion produces a larger value of s_u and a lower value of τ_{cyc}/s_u. Consequently, it appears that cyclic tests for soils that exhibit strain-hardening in monotonic undrained shearing are best interpreted in terms of a CRR rather than a τ_{cyc}/s_u ratio.

Effect of an initial static shear stress

The effect of an initial horizontal static shear stress (τ_{st}) on the cyclic undrained loading behavior for stratum A specimens is illustrated in Fig. 10, showing stress–strain responses for OCR = 1 specimens consolidated with τ_{st}/σ'_{vc} of 0.02, 0.05, and 0.10 prior to uniform cyclic loading with τ_{cyc}/σ'_{vc} = 0.225. The rate of shear strain accumulation increased progressively with increasing values of τ_{st}/σ'_{vc}; for example, the number of loading cycles to reach γ_{peak} = 5% decreased from nine cycles at τ_{st}/σ'_{vc} = 0.02 to only two cycles at τ_{st}/σ'_{vc} = 0.10. This behavior is consistent with those observed for other cohesive soils (e.g., Goulois et al. 1985; Andersen et al. 1988) and primarily reflects the fact that increasing the τ_{st} brings the peak shear stress ($\tau_{peak} = \tau_{st} + \tau_{cyc}$) closer to the soil's s_u.

Results of cyclic tests on stratum A specimens with τ_{st}/σ'_{vc} = 0.0 and $\tau_{st}/\sigma'_{vc} > 0$ are summarized in Fig. 11, showing the peak strength ratio (τ_{peak}/s_u) versus N to cause γ_{peak} = 3%. Test results for $\tau_{st}/\sigma'_{vc} > 0$ give similar, or slightly greater, peak strength ratios than were obtained for τ_{st}/σ'_{vc} = 0, regardless of specimen OCR. This trend may be partly attributed to the fact that consolidation under a τ_{st} generally causes an increase in s_u, whereas τ_{peak}/s_u is computed using the s_u for τ_{st}/σ'_{vc} = 0. These limited results are consistent with trends evident in other datasets (Goulois et al. 1985; Andersen et al. 1988).

Fig. 10. Effect of static shear stress on the stress–strain response of stratum A specimens during cyclic DSS loading.

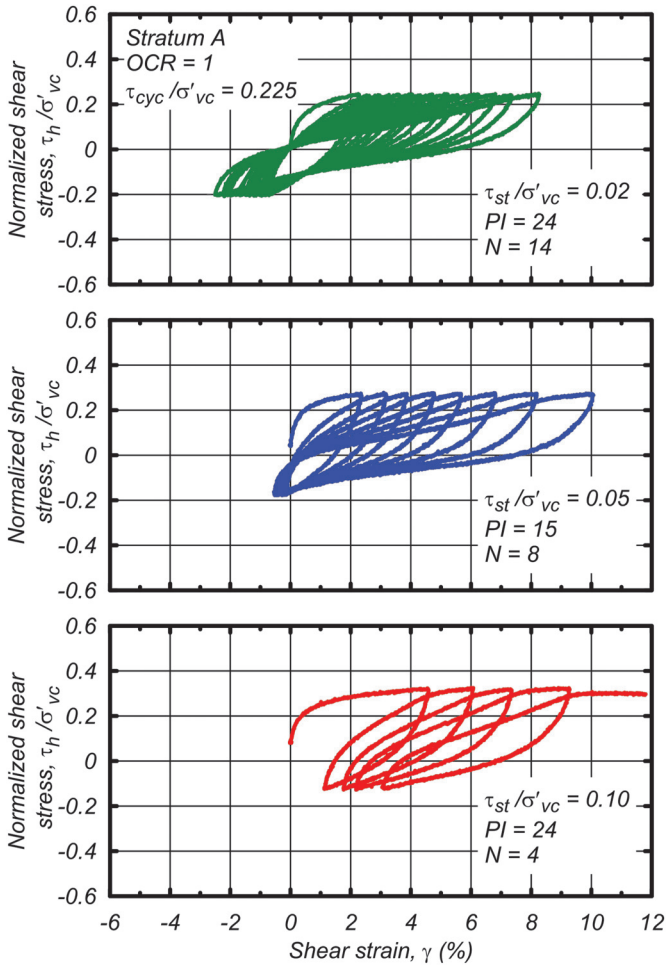

Fig. 11. Peak cyclic strength ratio to cause cyclic failure versus number of uniform loading cycles for stratum A specimens.

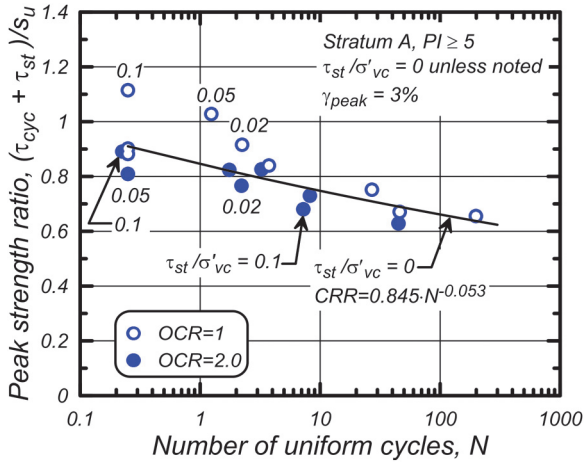

Post-cyclic reconsolidation strains

Post-cyclic reconsolidation strains were measured on eight of the cyclic test specimens from stratum A. At the end of cyclic

undrained loading, the specimens were brought back to their initial horizontal shear stress while maintaining undrained conditions. The specimens were then allowed to reconsolidate under vertical strain control until the effective vertical stress, σ'_v, equaled the initial σ'_{vc} value.

A typical test result showing the variation in void ratio versus σ'_v during both the initial consolidation and post-cyclic reconsolidation phases is shown in Fig. 12. This specimen was initially consolidated to σ'_{vc} = 480 kPa (with τ_{st} = 0), and then unloaded to σ'_{vc} = 240 kPa to produce an OCR = 2.0. The virgin compression index (C_c) was about 0.19 during the initial loading and the recompression index (C_r) was about 0.031 during the unloading. The specimen was then subjected to cyclic undrained loading at τ_{cyc}/σ'_{vc} of 0.40 until the specimen reached γ_{peak} = 5.4%. The cyclic undrained loading did not change the specimen's void ratio, but had reduced σ'_v to about 100 kPa (i.e., r_u = 0.56). Post-cyclic reconsolidation to σ'_v = 240 kPa produced a volumetric strain of 0.8% and a post-cyclic recompression index (C_{dyn}) of 0.047.

Post-cyclic volumetric strains for OCR = 1 specimens (three tests, PI = 24–26, $r_{u,max}$ = 0.69–0.78, τ_{st}/σ'_{vc} = 0.0–0.10) ranged from 1.7% to 2.5% and for OCR = 2.0 specimens (five tests, PI = 5–15, $r_{u,max}$ = 0.56–0.85, τ_{st}/σ'_{vc} = 0.0–0.10) ranged from 0.8% to 1.7%. Volumetric strains generally increased with increasing $r_{u,max}$ and decreased with increasing OCR, while possible effects of PI or τ_{st}/σ'_v were unclear. The OCR = 1 specimens had $C_r \approx 0.044$, C_{dyn} = 0.052–0.075, and C_{dyn}/C_r = 1.2–1.7. The OCR = 2.0 specimens had smaller C_r values (0.018–0.031) and smaller C_{dyn} values (0.033–0.047), but slightly larger C_{dyn}/C_r ratios (1.5–2.2). These post-cyclic volumetric strains and C_{dyn}/C_r ratios are comparable to values reported for similar soils under similar loadings (e.g., Ohara and Matsuda 1988; Fiegel et al. 1998).

Post-cyclic monotonic undrained strengths

Post-cyclic monotonic undrained DSS tests were performed on 13 specimens from stratum A and seven specimens from stratum B. At the end of cyclic loading, the specimens were returned to their undeformed positions before commencing the monotonic shearing. No drainage (consolidation) was allowed between the cyclic and monotonic undrained loading test phases. Strain rates during post-cyclic monotonic shearing were 5%/h for 11 tests and 50%/h in the other nine tests; the effects of strain rate were not evident within the variability of the experimental data.

Typical post-cyclic monotonic stress–strain responses for stratum A specimens (two at OCR = 1, three at OCR = 2.0) consolidated with τ_{st}/σ'_{vc} = 0 are shown in Fig. 13. The initial stress–strain responses are relatively soft until the imposed γ approaches the γ_{peak} that had developed during cyclic loading ($\gamma_{pk,cyc}$). Thus, the initial stiffness during post-cyclic monotonic loading decreases with increasing values of $\gamma_{pk,cyc}$, as expected. The shear resistances at shear strains greater than $\gamma_{pk,cyc}$ progressively increase until they become comparable to those measured in virgin monotonic undrained DSS tests. For example, the post-cyclic peak shear strengths for the stratum A specimens were 91% and 96% of the expected monotonic s_u for the two OCR = 1 tests and between 75% and 100% of the expected monotonic s_u for the three OCR = 2.0 tests. The ratio of post-cyclic monotonic to monotonic shear strengths did, however, decrease with increasing $\gamma_{pk,cyc}$, as shown in Fig. 14.

Typical post-cyclic monotonic stress–strain responses for the stratum B specimens (three at OCR = 1, one at OCR = 2.0) are shown in Fig. 15. The two specimens with PI ≥ 7 exhibited nearly perfectly plastic stress–strain responses similar to those of the more plastic stratum A soils, whereas the two nonplastic specimens (PI = 0) exhibited strain-hardening behavior to $\gamma \approx 20\%$. This difference in post-cyclic monotonic stress–strain behavior for nonplastic versus PI ≥ 7 specimens is similar to the differences observed in virgin monotonic undrained responses (Fig. 4). The ratio of post-cyclic

Fig. 12. CRS consolidation and reconsolidation curve for stratum A specimen.

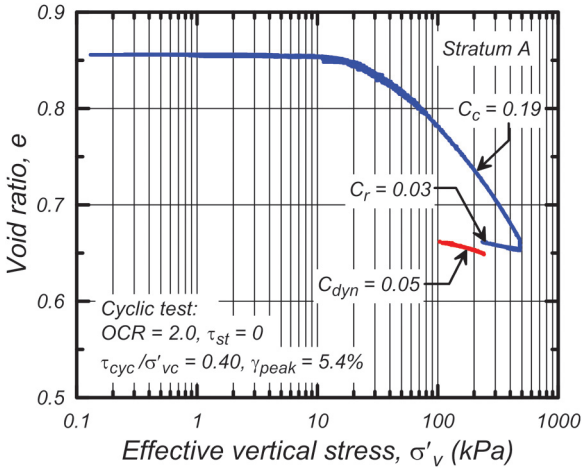

Fig. 13. Post-cyclic stress–strain response for stratum A specimens during undrained monotonic DSS.

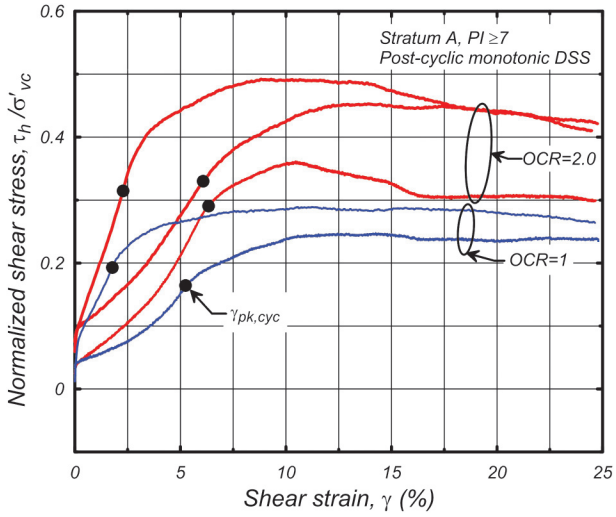

Fig. 14. Post-cyclic undrained strength loss relationship to peak cyclic shear strain and *N*.

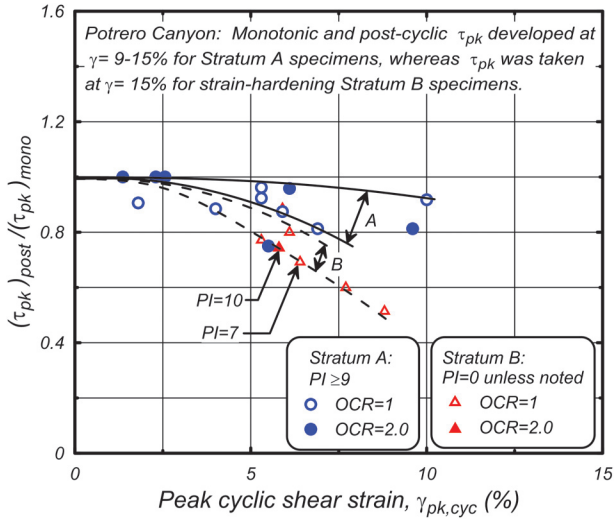

Fig. 15. Post-cyclic stress–strain response for stratum B specimens during undrained monotonic DSS loading.

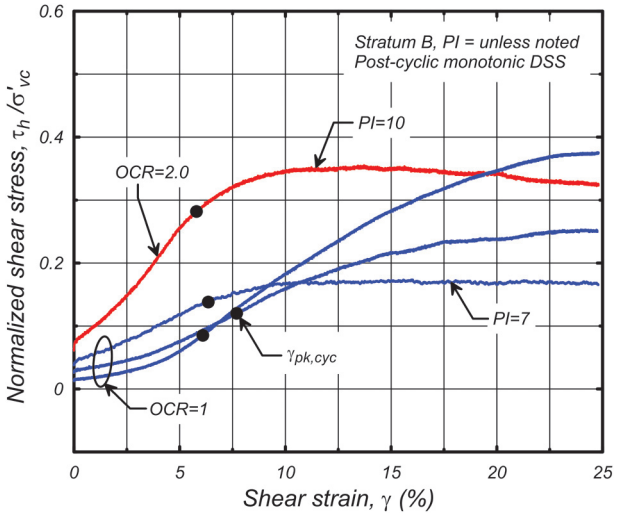

monotonic to monotonic shear strengths also decreased with increasing $\gamma_{pk,cyc}$, as shown in Fig. 14, with the ratios being lower for stratum B specimens than for stratum A specimens.

Discussion

The laboratory and field data for stratum A soils suggest that their in situ cyclic loading behavior under the proposed fills can be reasonably evaluated using laboratory testing. The data indicate that these soils are amenable to a stress-history normalization framework and have properties consistent with empirical correlations for sedimentary clays. This conclusion is consistent with guidance provided by the index test–based liquefaction susceptibility criteria of Bray and Sancio (2006) and Boulanger and Idriss (2006). The Bray and Sancio criteria indicate 9% of the samples are potentially liquefiable (PI ≤ 12 and $w_c \geq 0.85$LL) and another 11% are systematically more resistant to liquefaction, but still susceptible to cyclic mobility (12 ≤ PI ≤ 20 and $w_c \geq 0.80$LL). The Boulanger and Idriss criteria indicate only 3% are potentially liquefiable (i.e., are better evaluated using SPT-, CPT- or shear wave velocity (V_s)-based liquefaction triggering correlations rather than lab tests). The CPT-based correlation of Robertson and Wride (1998) indicates 18%–22% of the stratum is liquefiable based on a soil behavior type index (I_c) less than 2.6. The guidance provided by these index- and CPT-based correlations are consistent with the conclusion that laboratory testing of field samples can be used to assess the in situ cyclic loading behavior of these soils.

Measured cyclic strengths for stratum A are also consistent with empirical laboratory test–based correlations for plastic silts and clays. For example, the measured $CRR_{N=30,\gamma=3\%}$ values of 0.195 and 0.317 for OCR = 1 and 2.0, respectively, are close to the values of 0.180 and 0.338 estimated for OCR = 1 and 2.0 using the empirical correlation developed by Boulanger and Idriss (2007). The measured $(\tau_{cyc}/s_u)_{N=30,\gamma=3\%} = 0.71$ for OCR = 1.0 and 2.0 specimens (Fig. 9) is lower than the typical value of 0.83, but within the range of empirical data reported in Boulanger and Idriss (2007).

The laboratory and field data for stratum B soils need to be interpreted within the intended contexts of existing guidance. The laboratory test results suggest that these soils still show a strong dependence on stress history, but some aspects of behavior are similar to those commonly associated with cohesionless soils (e.g., strain-hardening responses during monotonic undrained shear). The liquefaction susceptibility criteria of Bray and Sancio (2006) would classify 100% of the samples as potentially liquefiable, whereas the criteria by Boulanger and Idriss (2006) would classify 88% as potentially liquefiable. The CPT-based correlation of Robertson and Wride (1998) would classify only 12% to 33% of the stratum as potentially liquefiable. The conclusion that these soils are potentially liquefiable leads to the inference that, as for clean sands, sampling disturbance may render the results of cyclic laboratory tests unreliable and thus, in situ cyclic loading behavior is best evaluated using SPT-, CPT-, or V_s-based liquefaction triggering correlations. Laboratory testing of field samples may, however, still provide reasonable measures of expected in situ behavior for the young, noncemented, compressible soils of this stratum because the future field-loading conditions will increase the consolidation stresses to values much greater than currently exist in situ. Consolidating laboratory samples to the future field stresses may mitigate the effects of sampling disturbance on cyclic testing behavior such that a laboratory testing program may still provide valuable information, as discussed below.

The measured cyclic strengths for normally consolidated stratum B specimens with PI < 7 were in the range of estimates obtained using CPT- and SPT-based liquefaction correlations for cohesionless soils and smaller than values estimated using the empirical laboratory test–based correlations for more plastic silts and clays. For example, the cyclic test results (Fig. 8) indicate $CRR_{\gamma=3\%}$ of 0.130 and 0.118 at 15 and 30 equivalent uniform loading cycles, respectively, after applying a reduction of 10% for the effects of bi-directional shaking. This $CRR_{N=15,\gamma=3\%}$ value is slightly greater than the $CRR_{M=7.5}$ estimates of 0.121 and 0.107 obtained using the CPT-based liquefaction triggering correlations of Robertson and Wride (1998) and Idriss and Boulanger (2008), respectively, and slightly smaller than the $CRR_{M=7.5}$ estimate of 0.149 obtained using an overburden- and energy-corrected SPT blow count, $(N_1)_{60}$, value of 9 representative of loose critical lenses within the stratum and the SPT-based correlation of Idriss and Boulanger (2008). At the same time, the laboratory-derived $CRR_{N=30,\gamma=3\%}$ value is smaller than the range of values (0.170–0.234) reported for silts and clays with PI = 10–27 in Boulanger and Idriss (2007). These comparisons indicate that the laboratory tests on field samples were producing estimates of in situ behavior consistent with the CPT- and SPT-based liquefaction correlations.

The cyclic testing of stratum B specimens, nonetheless, provided several important benefits that could not have been obtained otherwise. These benefits included obtaining data describing the post-earthquake reconsolidation behavior, the effect of initial static shear stresses on asymmetric strain accumulation during cyclic loading, and the relative effect that overconsolidation has on cyclic and monotonic strengths for use in evaluating the potential benefits of surcharging at the site. These types of data were particularly valuable for calibrating nonlinear constitutive models used in dynamic deformation analyses.

Conclusions

The results of the site characterization work for this recent Holocene alluvial silt and clay deposit produced comprehensive datasets for two strata that have characteristics spanning those commonly associated with liquefiable and nonliquefiable soils. Stratum A is predominantly composed of very soft clay and very loose silt with PI = 5 to 27, whereas stratum B is predominantly composed of very loose silty sand and sandy silt with PI = 0 to 10.

The laboratory and field data for stratum A soils suggest that their cyclic loading behavior can be reasonably evaluated using laboratory test–based procedures. The same conclusion is reached based on the index test–based liquefaction susceptibility criteria of Bray and Sancio (2006) and Boulanger and Idriss (2006) and the CPT-based liquefaction susceptibility criteria of Robertson and Wride (1998). The monotonic and cyclic strengths measured in DSS for OCR = 1 or 2.0 specimens are also in reasonable agreement with the empirical correlations developed by Boulanger and Idriss (2007).

The laboratory and field data for stratum B soils show aspects of behavior that are intermediate to those commonly associated with cohesive and cohesionless soils. The same index- and CPT-based liquefaction criteria described above indicate that these soils should be classified as liquefiable and their in situ cyclic strengths estimated using SPT-, CPT-, or V_s-based liquefaction triggering correlations. The use of laboratory tests to assess the in situ cyclic loading behavior of these young, noncemented, compressible soils was considered feasible because the future field consolidation stresses, and hence laboratory consolidation stresses, greatly exceeded the current in situ stresses. This conclusion is supported by the reasonable agreement between values of cyclic strength measured in DSS for OCR = 1 specimens and estimated using case history–based CPT and SPT liquefaction correlations.

The detailed field and laboratory testing studies for these two strata provided a number of benefits for the design of earthworks at this site beyond the questions of liquefaction susceptibility and cyclic strengths. These benefits included obtaining data describing (*i*) the post-earthquake reconsolidation behavior for estimating settlements, (*ii*) the effect of initial static shear stresses on asymmetric strain accumulation during cyclic loading, and (*iii*) the relative effect that overconsolidation from surcharging can have on cyclic and monotonic strengths. The data were particularly valuable in that they provided a basis for calibrating the nonlinear constitutive model used in the dynamic deformation analyses.

Acknowledgements

The field and initial laboratory testing was performed as part of a study by ENGEO, Inc. Support for additional laboratory testing was provided by a United States Society on Dams scholarship and the California Department of Water Resources. Assistance in performing laboratory tests was provided by Richard Fernandez and Sara Magallon. D.J. DeGroot provided valuable suggestions regarding laboratory testing procedures. The authors appreciate the above support and assistance.

References

Andersen, K., Kleven, A., and Heien, D. 1988. Cyclic soil data for design of gravity structures. Journal of the Geotechnical Engineering Division, ASCE, **114**(5): 517–539. doi:10.1061/(ASCE)0733-9410(1988)114:5(517).

ASTM. 2011. Standard practice for classification of soils for engineering purposes (Unified Soil Classification System). ASTM standard D2487. American Society for Testing and Materials, West Conshohocken, Pa.

Bennett, M.J., Criley, C., Tinsley, J.C., III, Ponti, D.J., Holzer, T.L., and Conaway, C.J. 1998. Subsurface geotechnical investigations near sites of permanent ground deformation caused by the January 17, 1994 Northridge, California earthquake. U.S. Geological Survey Open-File Rep. 98-373. U.S. Geological Survey, Menlo Park, Calif.

Boulanger, R.W., and Idriss, I.M. 2006. Liquefaction susceptibility criteria for silts and clays. Journal of Geotechnical and Geoenvironmental Engineering, **132**(11): 1413–1426. doi:10.1061/(ASCE)1090-0241(2006)132:11(1413).

Boulanger, R.W., and Idriss, I.M. 2007. Evaluation of cyclic softening in silts and clays. Journal of Geotechnical and Geoenvironmental Engineering, **133**(6): 641–652. doi:10.1061/(ASCE)1090-0241(2007)133:6(641).

Boulanger, R.W., Meyers, M.W., Mejia, L.H., and Idriss, I.M. 1998. Behavior of a fine-grained soil during the Loma Prieta earthquake. Canadian Geotechnical Journal, **35**(1): 146–158. doi:10.1139/t97-078.

Bray, J.D., and Sancio, R.B. 2006. Assessment of the liquefaction susceptibility of fine-grained soils. Journal of Geotechnical and Geoenvironmental Engineering, **132**(9): 1165–1177. doi:10.1061/(ASCE)1090-0241(2006)132:9(1165).

Chandler, R.J. 1988. The in-situ measurement of the undrained shear strength of clays using the field vane. *In* Vane shear strength testing in soils. *Edited by* A.F. Richards. ASTM STP 1014. American Society for Testing and Materials (ASTM). pp. 13–44.

Dahl, K.R. 2011. Evaluation of seismic behavior of intermediate and fine-grained soils. Doctoral thesis, University of California, Davis.

DeGroot, D.J., Germaine, J.T., and Ladd, C.C. 1994. Effect of nonuniform stresses on measured DSS stress-strain behavior. Journal of Geotechnical and Geoenvironmental Engineering, **120**(5): 892–912. doi:10.1061%2F%28ASCE%290733-9410%281994%29120%3A5%28892%29.

Fiegel, G.L., Kutter, B.L., and Idriss, I.M. 1998. Earthquake-induced settlement of soft clay. *In* Proceedings of Centrifuge 98. Balkema, Rotterdam. Vol. 1, pp. 231–236.

Goulois, A.M., Whitman, R.V., and Hoeg, K. 1985. Effects of sustained shear stresses on the cyclic degradation of clay. *In* Strength testing of marine sediments: laboratory and in-situ strength measurements. *Edited by* R.C. Chaney and K.R. Demars. ASTM STP 883. ASTM, Philadelphia, Pa. pp. 336–351.

Hight, D., and Leroueil, S. 2003. Characterization of soils for engineering purposes. A.A. Balkema, USA. pp. 255–360.

Holzer, T.L., Bennett, M.J., Ponti, D.J., and Tinsley, J.C., III. 1999. Liquefaction and soil failure during 1994 Northridge earthquake. Journal of Geotechnical and Geoenvironmental Engineering, **125**(6): 438–452. doi:10.1061/(ASCE)1090-0241(1999)125:6(438).

Idriss, I.M., and Boulanger, R.W. 2008. Soil liquefaction during earthquakes. Monograph MNO-12. Earthquake Engineering Research Institute, Oakland, Calif.

Ladd, C.C. 1991. Stability evaluation during stage construction. Journal of Geotechnical and Geoenvironmental Engineering, **117**(4): 540–615. doi:10.1061%2F%28ASCE%290733-9410%281991%29117%3A4%28540%29.

Ladd, C.C., and Foott, R. 1974. New design procedure for stability of soft clays. Journal of the Geotechnical Engineering Division, ASCE, **100**(GT7): 763–786. doi:10.1016%2F0148-9062%2874%2990494-X.

Lunne, T., and Kleven, A. 1981. Role of CPT in North Sea foundation engineering. *In* Cone Penetration Testing and Experience. ASCE. pp. 76–107.

Lunne, T., Berre, T., and Strandvik, S. 1997. Sample disturbance effects in soft low plasticity Norwegian clay. *In* Proceedings, Conference on Recent Developments in Soil and Pavement Mechanics, Rio de Janeiro, Brazil. pp. 81–102.

Ohara, S., and Matsuda, H. 1988. Study on the settlement of saturated clay layer induced by cyclic shear. Soil and Foundations, **28**(3): 103–113. doi:10.3208/sandf1972.28.3_103.

Randolph, M.F. 2004. Characterization of soft sediments for offshore applications. Keynote Lecture. *In* Proceedings, 2nd International Conference on Site Characterization, Porto. Vol. 1, pp. 209–231.

Robertson, P.K., and Wride, C.E. (Fear). 1998. Evaluating cyclic liquefaction potential using the cone penetration test. Canadian Geotechnical Journal, **35**(3): 442–459. doi:10.1139/t98-017.

Rymer, M.J., Fumal, T.E., Schwartz, D.P., Powers, T.J., and Cinti, F.R. 1995. Distribution and recurrence of surface fractures in Potrero Canyon associated with the 1994 Northridge, California, earthquake. *In* The Northridge, California, earthquake of 17 January 1994. *Edited by* M.C. Woods and W.R. Seiple. Special Publication 116. California Division of Mines and Geology, Sacramento, Calif., pp. 133–146.

Sanin, M.V., and Wijewickreme, D. 2006. Cyclic shear response of channel-fill Fraser River Delta silt. Soil Dynamics and Earthquake Engineering, **26**: 854–869. doi:10.1016/j.soildyn.2005.12.006.

Terzaghi, K., Peck, R.B., and Mesri, G. 1996. Soil mechanics in engineering practice. John Wiley and Sons, New York.

Yilmaz, M.T., Pekcan, O., and Bakir, B.S. 2004. Undrained cyclic shear and deformation behavior of silt-clay mixtures of Adapazari, Turkey. Soil Dynamics and Earthquake Engineering, **24**: 497–507. doi:10.1016/j.soildyn.2004.04.002.